Journal of the European Ceramic Society **19** (1999) 2021–2026

PII: S0955-2219(99)00005-9
0955-2219/99/$ - see front matter

Structural Data from X-ray Powder Diffraction of a New Phase Formed in the Si_3N_4–La_2O_3–Y_2O_3 System After Oxidation in Air

F. Monteverde* and G. Celotti

Research Institute for Ceramics Technology, Via Granarolo, 64–48018 Faenza (RA), Italy

(Received 12 November 1998; accepted 12 December 1998)

Abstract

A new phase formed at high temperature with composition $(Y_{2/3}La_{1/3})_2Si_2O_7$ was found among the reaction products of a hot pressed Si_3N_4-based material (with Y_2O_3 and La_2O_3 as sintering aids) after oxidation experiments. This phase was also directly synthesized from oxide precursors (SiO_2, Y_2O_3, La_2O_3) at 1600°C, under the condition of a silica excess. After identifying a proper monoclinic cell, the structure of such a compound was successfully refined by Rietveld method starting from the existing model of G-form of $La_2Si_2O_7$. The new phase turned out to be isostructural with it, showing however a characteristic inhomogeneous substitution of Y atoms by La ones in only half the cell positions and a rather distorted arrangement of Si–O tetrahedra. © *1999 Elsevier Science Limited. All rights reserved*

Keywords: powders — solid state reaction, X-ray method, silicates, Si_3N_4, Rietveld refinement.

1 Introduction

Silicon nitride (SN) based materials attracted great attention for the ability to retain their intrinsic stability and to exhibit high performance mechanical properties at high temperatures (HT).[1,2]

Fully dense SN-based materials can be produced by liquid phase sintering (LPS), which is activated by the addition of metal oxides (i.e. MgO, Al_2O_3, Y_2O_3, La_2O_3, CeO_2, etc.) to the SN raw powders. The design of the initial mixture together with an appropriate tuning of the process parameters allows control fine densification and grain growth during LPS, and consequently the development of tailored microstructures. The properties of the as-sintered materials are directly dependent upon the characteristics of the grain boundary (GB) phases formed from liquid phase during cooling. Furthermore the microstructural stability must be retained during HT applications and not be degraded by environmental interactions (i.e. oxidation, corrosion, etc.).[2,3]

The oxidation resistance of the multiphase SN ceramics is strongly influenced by the type and content of their secondary phases. After oxidation tests reaction products, formed on the surface, are generally constituted of silica (from the direct oxidation of the SN matrix) and different silicate(s).[3] The latter arises from the reaction between the silica and the additives/impurities which, from the inner bulk, are diffused into the outer silica growing scale.[4]

The present study aims to identify the stoichiometry and to solve the crystallographic structure of a new silicate formed during oxidation within the surface reaction scale (Fig. 1) of an SN-based material hot-pressed with Y_2O_3 and La_2O_3 as sintering aids.[5] In fact, after oxidation tests at temperatures higher than 1400°C, XRD analyses on oxidised surfaces detected systematically a crystalline compound (labelled YLaSiO) not yet listed in the ICDD files.

2 Experimental

Detailed description of processing procedures and properties of the SN/La_2O_3/Y_2O_3 material were reported elsewhere.[5] Oxidation tests on as-sintered samples over a wide temperature range (1000–1500°C) were performed:[4] only from 1400°C XRD patterns from oxidised surfaces clearly indicated the presence of the new compound YLaSiO.

*To whom correspondence should be addressed.

Several attempts were carried out to synthesize from oxide precursors (SiO_2, Y_2O_3, La_2O_3) the YLaSiO phase: only an excess of amorphous silica in the initial mixture was revealed to be the key condition to successfully obtain the expected YLaSiO phase in satisfactory amounts. A great deal of effort was spent in synthesizing the desired compound with a powdered character in order to eliminate some features which might interfere with the structural and chemical inspection of this new phase: the set of β-SN peaks, the textured growth of YLaSiO phase in the oxidation scale, the graduated (ie. not random) arrangement of the phases present throughout the reaction scale (Fig. 2).

In Table 1 are schematized the process parameters of the synthesis test.

The final pellet, processed from $SiO_2/Y_2O_3/La_2O_3$ precursors, was ground finely with an agate mortar and the XRD studies were conducted on the relative powdered sample.

Accurate XRD patterns were recorded over an angular range $10° < 2\theta < 60°$ on a Rigaku Miniflex powder diffractometer with CuK_α radiation, employing a 2θ step width of 0·02° and a step counting time of 10 s. The experimental diffraction data were processed using the following programs: TREOR-5[6] to find elementary cells, DBWS-9411[7] to perform Rietveld refinement, DMPLOT[8] and POWDER CELL[9] for the necessary graphic representations.

3 Results and discussion

Figures 1 and 3 show, respectively, a typical micrograph of an oxidized surface of the hot-pressed Si_3N_4–Y_2O_3–La_2O_3 sample and the relative XRD pattern. In the bright areas is located the investigated phase, embedded in a silica-rich glassy scale which represents the main reaction product of the oxidation process. α-cristobalite (well indicated in the XRD pattern) is mainly placed at the oxide scale/unreacted bulk interface of the sample (Fig. 4).

Figure 5 shows the XRD pattern of the final powder (obtained from the oxide precursors) where, besides the presence of α-cristobalite (ICDD file

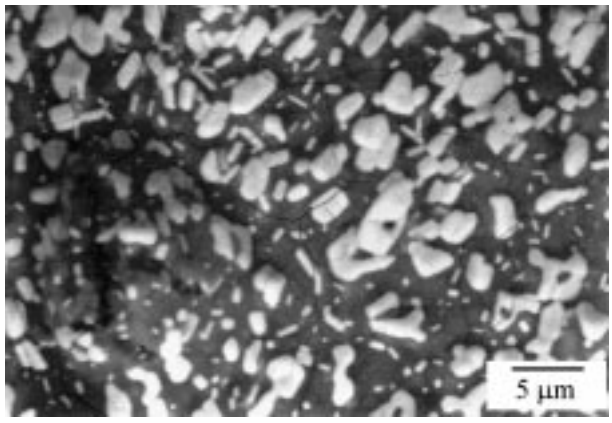

Fig. 1. SEM micrograph by backscattered electrons (BSE) from an oxidised surface of hot pressed $Si_3N_4/La_2O_3/Y_2O_3$ material.

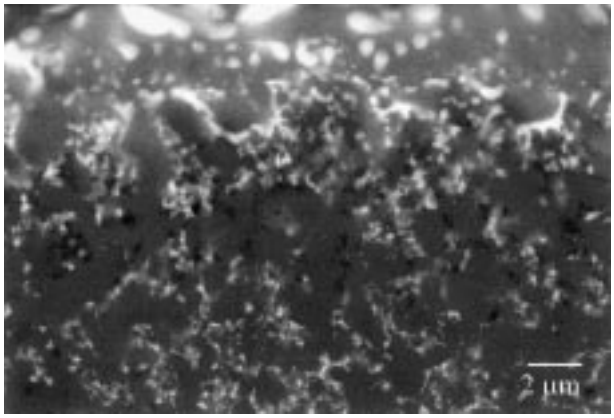

Fig. 2. SEM micrograph by BSE from polished cross section of hot-pressed $Si_3N_4/La_2O_3/Y_2O_3$ oxidised material: the gradual microstructural transition from the oxidised surface (upper) to the unreacted bulk (lower) is evidenced.

Table 1. Experimental setup of process parameters for the synthesis of the new phase

Raw powders	SiO_2 Carlo Erba, amorphous, Italy La_2O_3 Merck, Germany Y_2O_3 HCST grade C, Germany
Composition (wt%)	SiO_2 (70); La_2O_3 (15); Y_2O_3 (15)
Powder treatment	a. SiO_2 softly pestled in agate mortar b. Mixing of the oxide precursors in ethanol by pulsed ultrasonicator c. Dried in rotovapor (85°C)
Thermal cycle	a. Pellettized and mounted on a Pt support b. 1600°C for 2 h in laboratory static air, 300°C/h c. Crushed the pellet in agate mortar d. Small addition of fresh mixture, repeat (a) e. Repeat (b) for 6 h

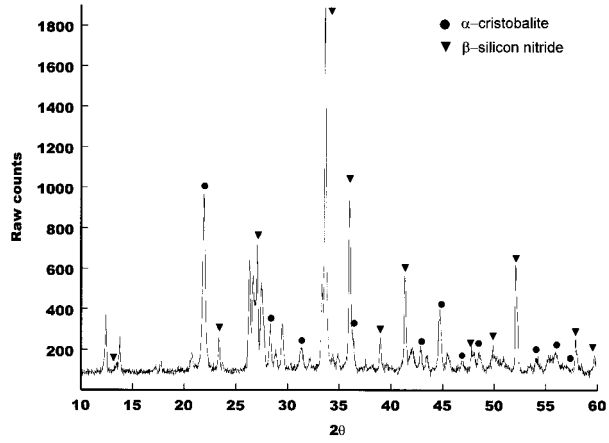

Fig. 3. XRD pattern from oxidized surface of hot-pressed $Si_3N_4/La_2O_3/Y_2O_3$ material. Unmarked peaks belong to the new phase.

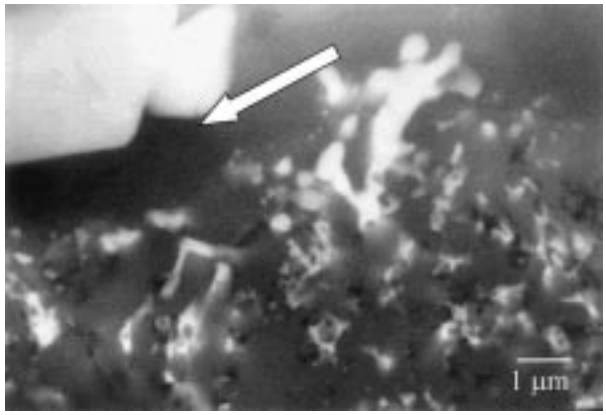

Fig. 4. SEM micrograph by BSE from polished cross section of hot-pressed $Si_3N_4/La_2O_3/Y_2O_3$ oxidised material: the arrow indicates the preferential location of α-cristobalite at the oxide scale (upper) /unreacted bulk (lower) interface.

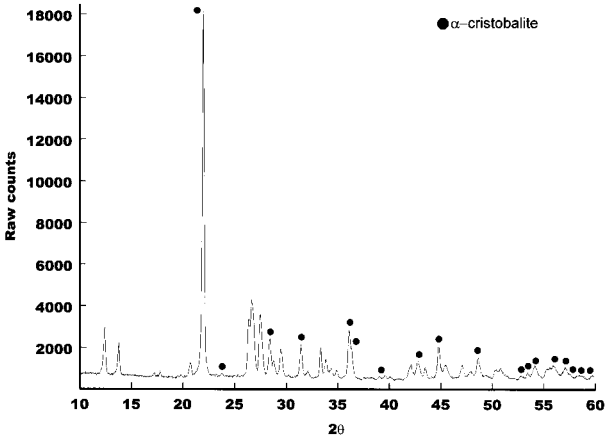

Fig. 5. XRD pattern of the YLaSiO/α-cristobalite powder mixture, synthesized as reported in Table 1. Unmarked peaks belong to YLaSiO phase.

39-1425), a sequence of unknown peaks are present. The morphological examination (by SEM) of such a powder evidenced grey blocks (α-cristobalite) upon which the new formed phase (bright spots) is anchored (Fig. 6): this feature, assessed the synthesis of YLaSiO cannot prescind from a silica excess. No unreacted precursors (Y_2O_3, La_2O_3) were found.

No known compound was able to account, besides α-cristobalite, for the unindexed observed reflections in Fig. 5: after a careful inspection, a Lanthanum disilicate, $La_2Si_2O_7$, was found[10,11] with a powder diffractogram remarkably similar, apart from systematically larger interplanar spacing values. Considering that quantitative EDX analyses provided for the new compound a composition near to $(Y_{2/3}La_{1/3})_2Si_2O_7$, an immediate deduction was to identify it as an analogous silicate with a partial substitution of La atoms to Y ones. This hypothesis supplied a good starting model for structural analysis, avoiding the uncertainties connected to any ab-initio determination.

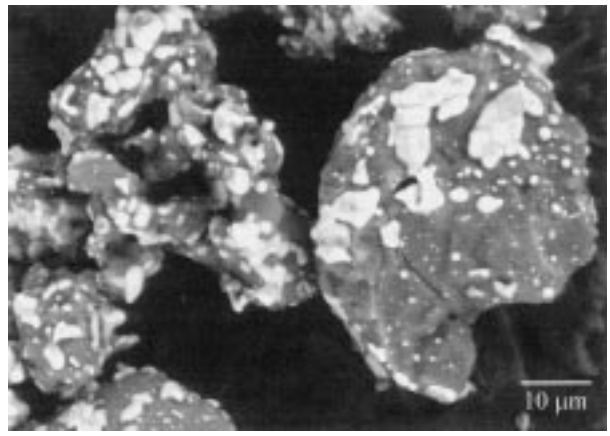

Fig. 6. SEM micrograph by BSE of the final powder, synthesized as reported in Table 1.

The first step was the evaluation of reasonably reliable cell parameters and consequently of the crystallographic system. The task was accomplished by TREOR 5 routine[6] that yielded, as unique cell with satisfactory figure of merit (20), a monoclinic one with $a = 5{\cdot}367$, $b = 8{\cdot}549$, $c = 13{\cdot}855$Å, $\beta = 111{\cdot}73°$. These values turned out to be very close to those of Greis et al.[11] for G-form of $La_2Si_2O_7$: practically coincident β angle, a less than 1% shorter and b and c about 2·5% smaller.

This structure appears as a monoclinic distortion of δ-$Y_2Si_2O_7$, an orthorhombic disilicate belonging to the group of α-$Ca_2P_2O_7$.[12] Furthermore such a cell, if containing four units of the hypothesized stoichiometry, would give a density of about 4·25 g cm^{-3}, in fairly good proportion with the value found for the pure Lanthanum disilicate. After a complete indexing of the observed pattern, the following systematic absences were identified: ($h0l$) with $l = 2n + 1$, ($0k0$) with $k = 2n + 1$ and ($00l$) with $l = 2n + 1$ (the last a consequence of the first one), clearly indicating $P2_1/c$ (14) as the most probable space group with all atoms in general positions.

On the basis of this cell, a Rietveld refinement was attempted starting from the atomic coordinates of Greis *et al.* model[11] and introducing the vicariance 2/3Y + 1/3La in the heavy atoms positions. The DBWS-9411 program[7] was employed in PC version: moreover, owing to the impossibility of synthesizing the pure phase (i.e. in absence of SiO_2 excess), the well known data of tetragonal α-cristobalite were introduced in the refinement procedure as well.

The experimental XRD data, to be processed by the Rietveld method, were collected according to the strategy illustrated by Hill,[13] and a powder diffractogram of pure, similarly prepared, α-cristobalite was also recorded in comparable conditions to make easier any further handling.

The results of whole-powder-pattern fitting (plotted by DMPLOT program[8]) are presented in Fig. 7: reliability indices R_p and R_{wp} and the goodness-of-fit index S were 4·9%, 6·6% and 2·0, respectively.

The structural data of the YLaSiO phase are reported in Table 2 and the diffraction data are summarized in Table 3. Figure 8 shows a projection of the YLaSiO monoclinic structure along [100] at $(10\bar{1})$, obtained by the PowderCell program.[9]

From the data reported in Table 2 some aspects can be emphasized: even if the refinement started with La atoms systematically distributed (according to the stoichiometric proportion) in both lanthanide Ln(1) and Ln(2) positions, any further improvement in the structural fit was gained with all La atoms in position Ln(1), leaving position Ln(2) fully occupied by Y atoms. Moreover, within the stoichiometric hypothesis of the model, the best fit implies not negligible displacements of some oxygen atoms from the geometrically regular tetrahedral positions. Such a distorted arrangement is likely due to the particular conditions in which the YLaSiO phase nucleates and grows: in fact, at the synthesis temperatures, the silica viscous 'substrate' turns out to be in a state far from the thermodynamic equilibrium, partially retained during cooling. The feature of the silica excess, as an essential starting point over which the desired reaction may proceed is once more confirmed. The attempts to synthesize the YLaSiO phase from stoichiometric (or nearly so) mixture of the oxide precursors regularly failed with the result of forming only simple Ln-silicates (Y_2SiO_5, $Y_2Si_2O_7$, La_2SiO_5, $La_2Si_2O_7$).

Furthermore some problems were encountered in adequately fitting conventional functions to a rather uneven background: clearly many additional non-crystalline scattering components are present, but the general features of our XRD pattern did not permit a meaningful Fourier-filtering of residual intensities[14] and therefore the refinement procedure was stopped at the reliability indices values previously reported.

It has to be noted that the lacking fit on the exceptionally strong main reflection of the α-cristobalite (Fig. 7), at least useful as internal standard, clearly worsens the overall reliability indices obtained but it does not affect significantly the refinement of the YLaSiO phase structure.

Table 2. Structural data of the new phase $(Y_{2/3}La_{1/3})_2Si_2O_7$[a]

Atom	*x*	*y*	*z*	*Occupancy factor*
Y(1)	0·5164	0·8065	0·7714	0·335
La(1)				0·665
Y(2)	0·8249	0·6019	0·5880	1
Si(1)	0·726	0·266	0·028	1
Si(2)	0·940	0·498	0·182	1
O(1)	0·857	0·454	0·084	1
O(2)	0·007	0·160	0·028	1
O(3)	0·621	0·134	0·070	1
O(4)	0·565	0·263	0·904	1
O(5)	0·767	0·497	0·257	1
O(6)	0·249	0·444	0·241	1
O(7)	0·035	0·680	0·169	1

[a]Monoclinic cell, space group $P2_{1/c}$ (14), $a = 5{\cdot}375(1)$ Å, $b = 8{\cdot}569(1)$ Å, $c = 13{\cdot}863(1)$ Å, $\beta = 111{\cdot}79(1)°$, $Z = 4$, $V = 592.9$ Å^3, $\rho = 4{\cdot}25$ g cm^{-3}, $B_{OV} = 0{\cdot}5$, $R_{wp} = 6{\cdot}6\%$, all atoms in general positions x,y,z (4e).

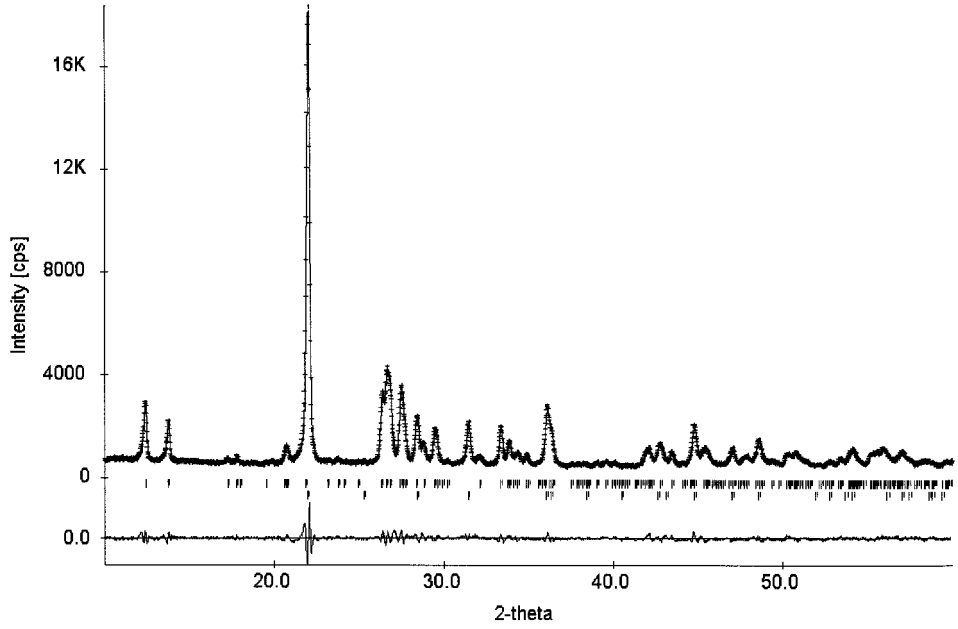

Fig. 7. Results of whole-powder-pattern fitting by Rietveld refinement for the investigated mixture (observed profile intensities (+) and calculated intensities (−): in the bottom diagram the difference plot between the observed and calculated intensities is shown). Short verticals bars represent the Bragg reflection positions of YLaSiO (upper) and α-cristobalite (lower).

Table 3. X-ray powder diffraction data of the new phase $(Y_{2/3}La_{1/3})_2Si_2O_7$. The intensity of the reflections belonging to α-cristobalite was carefully subtracted after cumulative refinement

h	k	l	d (Å)	I calc.	I obs.	h	k	l	d (Å)	I calc.	I obs.
0	1	1	7·133	711	702	1	1	5	1·9522	14	12
0	0	2	6·436	472	465	2	3	−1	1·9387	12	12
0	1	2	5·146	55	52	1	1	−7	1·9296	41	38
1	0	0	4·991	70	66	0	4	3	1·9166	20	19
1	0	−2	4·929	21	11	0	3	5	1·9124	12	12
1	1	−1	4·553	23	25	1	4	1	1·9047	102	94
1	1	0	4·313	15	13	1	4	−3	1·8977	128	119
0	2	0	4·285	124	122	2	3	0	1·8793	24	27
1	1	−2	4·272	27	27	2	2	2	1·8719	149	146
0	2	1	4·065	99	108	2	3	−4	1·8658	89	82
0	1	3	3·837	31	26	2	2	−6	1·8455	102	81
1	1	1	3·744	20	31	2	1	3	1·8324	21	13
1	1	−3	3·691	12	9	1	2	5	1·8159	133	136
0	2	2	3·567	25	21	1	4	2	1·8098	39	92
1	0	2	3·383	789	810	1	3	4	1·8093	43	
1	2	−1	3·350	1000	1000	2	1	−7	1·8016	17	37
1	0	−4	3·325	923	944	1	4	−4	1·8008	18	
1	2	0	3·251	698	730	0	1	7	1·7980	38	171
1	2	−2	3·234	513	523	1	2	−7	1·7977	134	
0	0	4	3·218	112	121	1	3	−6	1·7942	77	74
1	1	2	3·147	196	209	2	3	1	1·7895	37	37
1	1	−4	3·100	227	247	0	4	4	1·7833	35	37
0	2	3	3·032	484	468	3	0	−2	1·7787	28	29
0	1	4	3·013	82	85	2	3	−5	1·7721	58	49
1	2	1	2·985	15	13	3	1	−3	1·7536	7	5
1	2	−3	2·958	23	25	1	0	6	1·7495	25	13
0	3	1	2·789	119	130	3	1	−2	1·7416	8	5
2	0	−2	2·687	496	464	3	1	−4	1·7335	18	18
1	2	2	2·655	50	50	1	0	−8	1·7305	10	10
1	1	3	2·647	276	282	0	3	6	1·7154	11	12
1	2	−4	2·627	50	48	1	1	6	1·7141	102	123
0	3	2	2·611	63	178	0	5	1	1·6988	48	52
1	1	−5	2·610	135		1	4	3	1·6975	96	103
0	2	4	2·573	127	118	1	1	−8	1·6963	56	59
2	1	−2	2·564	24	20	2	0	4	1·6914	28	29
2	1	−1	2·523	22	8	0	2	7	1·6899	8	8
2	0	0	2·496	34	32	1	4	−5	1·6876	116	120
1	3	0	2·479	170	168	2	3	2	1·6819	16	17
1	3	−2	2·471	77	73	3	0	0	1·6638	61	155
0	1	5	2·466	55	64	2	4	−1	1·6635	97	
2	0	−4	2·464	14		2	3	−6	1·6627	5	43
2	1	0	2·396	28	21	2	0	−8	1·6623	39	
0	3	3	2·378	26	24	2	1	4	1·6594	27	90
1	3	1	2·355	38	32	2	4	−3	1·6587	63	
1	2	−5	2·308	6	61	3	2	−3	1·6528	170	181
1	0	−6	2·306	58		0	4	5	1·6467	65	71
2	2	−2	2·277	69	83	3	0	−6	1·6429	111	260
1	1	4	2·256	15	17	3	2	−2	1·6428	125	
2	2	−1	2·248	27	31	1	3	5	1·6410	12	13
1	3	−4	2·167	33	24	3	2	−4	1·6360	42	46
2	2	0	2·157	139	136	1	5	−1	1·6328	4	65
0	0	6	2·145	178	199	2	1	−8	1·6319	55	
0	3	4	2·136	12	78	1	3	−7	1·6275	32	38
2	2	−4	2·136	68		2	4	0	1·6255	6	7
0	4	1	2·113	354	351	1	2	6	1·6197	47	80
0	1	6	2·081	185	195	1	5	−2	1·6187	23	
2	0	2	2·081	10		3	1	−6	1·6135	26	27
1	2	4	2·052	29	9	1	2	−8	1·6046	21	24
0	4	2	2·033	46	65	3	2	−5	1·5946	9	12
1	2	−6	2·031	32		1	5	1	1·5847	70	73
2	2	1	2·024	375	453	1	5	−3	1·5806	84	81
2	1	2	2·022	79		1	4	4	1·5795	10	10
2	2	−5	1·9986	280	264	2	2	4	1·5732	9	10
1	3	3	1·9933	52	46	2	3	3	1·5679	5	6
1	4	−1	1·9900	24	106	2	4	1	1·5663	11	13
2	1	−6	1·9890	94		2	4	−5	1·5546	5	4
1	3	−5	1·9772	30	26	3	1	1	1·5512	29	30
1	4	0	1·9686	11	8	3	2	0	1·5509	4	
1	4	−2	1·9647	6	4	2	2	−8	1·5497	22	21
2	3	−2	1·9572	14	10	2	3	−7	1·5485	11	11
						0	3	7	1·5462	52	55

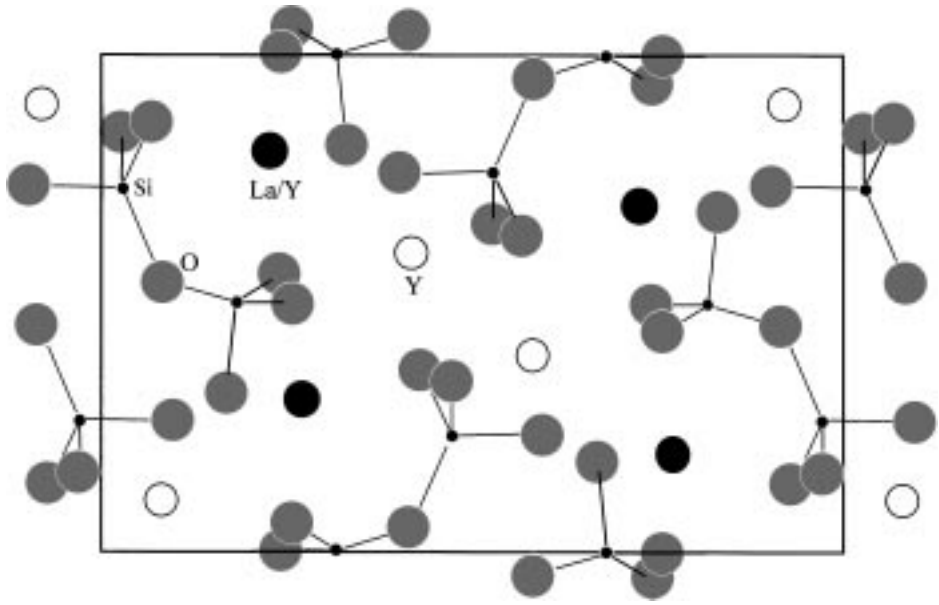

Fig. 8. Projection of the monoclinic $(Y_{2/3}La_{1/3})_2Si_2O_7$ structure seen along [100] at $(10\bar{1})$.

4 Conclusions

A new phase $(Y_{2/3}La_{1/3})_2Si_2O_7$ formed at high temperature was found in the reaction products of hot-pressed Si_3N_4 (added with 3 wt% Y_2O_3 + 3 wt% La_2O_3) after oxidation experiments. Attempts to synthesize this phase as pure compound failed because the presence of a noticeable silica excess proved to be necessary. However a mixture of α-cristobalite and the new phase was successfully obtained. Accurate XRD powder data were employed to carry out Rietveld analysis on the two-phase (YLaSiO and α-cristobalite) sample, starting from the structural model proposed by Greis et al.[11] for G-form of $La_2Si_2O_7$, whose pattern exhibited too many resemblances to be accidental. The refinement procedure, that could not be pushed further, mainly owing to the additional non-crystalline scattering contributions making it difficult to account properly for the background, yielded a monoclinic cell ($a = 5{\cdot}375$ $b = 8{\cdot}569$ and $c = 13{\cdot}863$Å, $\beta = 111{\cdot}79°$; space group $P2_1/c$ (14); $Z = 4$, $\rho = 4{\cdot}25$ g cm^{-3}) and atomic coordinates showed that substitution of La for Y atoms only occurs in half of the possible lattice positions, while Si–O tetrahedra appear somewhat distorted probably due to the very particular conditions of nucleation and growth.

Acknowledgements

The authors sincerely thank A. Bellosi for her skilful advice.

References

1. Gogotsi, Y. G. and Grathwohl, G., Stress enhanced oxidation of silicon nitride ceramics. *J. Am. Cer. Soc.*, 1993, **76**, 3093–3104.
2. Jacobson, N. S., Corrosion of silicon nitride ceramics in combustion environments. *J. Am. Cer. Soc.*, 1993, **76**, 3–28.
3. Nickel, K. G., Corrosion of non oxide ceramics. *Ceramics International*, 1997, **23**, 127–133.
4. Monteverde, F. and Bellosi, A., High oxidation resistance of hot pressed silicon nitride containing yttria and lanthania. *J. Eur. Cer. Soc.*, 1998, **18**(16), 2313–2321.
5. Bellosi, A., Monteverde, F. and Babini, G. N., Influence of powder treatment methods on sintering, microstructure and properties of Si_3N_4-based materials. In *Engineering Ceramics '96: Higher Reliability through Processing*, NATO ASI Series Vol. **25**, eds G. N. Babini, M. Haviar and P. Šajgalík, Kluwer Academic, Dordrecht, The Netherlands, 1997, pp. 197–212.
6. Werner, P. E., TREOR-5, *Trial and Error Program for Indexing of Unknown Powder Patterns*. University of Stockholm, Stockholm, 1988.
7. Young, R. A., Sakthivel, A., Moss, T. S. and Paiva-Santos, C. O., DBWS-9411, *Rietveld Analysis of X-ray and Neutron Powder Diffraction Patterns*. Georgia Institute of Technology, Atlanta, GA, 1995.
8. Marciniak, H., DMPLOT, *Plot View Program for Rietveld Refinement Method*. High Pressure Research Centre, Warsaw, 1995.
9. Kraus, W. and Nolze, G., *PowderCell for Windows 1·0*. Federal Institute for Materials Research and Testing, Berlin, 1997.
10. ICDD cards nos. 44-346 and 47-452. International Centre for Diffraction Data, Newtown Square.
11. Greis, O., Bossemeyer, H. G., Greil, P., Breidenstein, B. and Haase, A., Structural data of the monoclinic high-temperature G-form of $La_2Si_2O_7$ from X-ray powder diffraction. *Materials Science Forum*, 1991, **79–82**, 803–808.
12. Liddell, K. and Thompson, D. P., X-ray diffraction data from yttrium silicates. *Br. Ceram. Trans. J.*, 1986, **85**, 17–22.
13. Hill, R. J., Data collection strategies: fitting the experiment to the need. In *The Rietveld Method*, ed. R. A. Young IUCr/Oxford University Press, Oxford. 1995, pp. 61–101.
14. Richardson Jr, J. W., Background modelling in Rietveld analysis. In *The Rietveld Method*, ed. R. A. Young IUCr/Oxford University Press, Oxford, 1995, pp. 102–110.